Supporting Information

Comparative Study of Materials-Binding Peptide Interactions with Gold and Silver Surfaces and Nanostructures: A Thermodynamic Basis for Biological Selectivity of Inorganic Materials

J. Pablo Palafox-Hernandez,[1,#] Zhenghua Tang,[2,#] Zak E. Hughes,[1,#] Yue Li,[3] Mark T. Swihart,[3] Paras N. Prasad,[4,5] Tiffany R. Walsh,[1,*] and Marc R. Knecht[2,*]

[1]Institute for Frontier Materials, Deakin University, Geelong, Victoria 3216, Australia.

[2]Department of Chemistry, University of Miami, 1301 Memorial Drive, Coral Gables, Florida 33146, United States.

[3]Department of Chemical and Biological Engineering and [4]Department of Chemistry and Institute for Laser Photonics and Biophotonics, University at Buffalo (SUNY), Buffalo, New York 14260, United States.

5. Department of Chemistry, Korea University, Seoul 151-747, Korea

[#]These authors contributed equally.

*To whom correspondence should be addressed:

MK: Phone: (305) 284-9351, email: knecht@miami.edu; TRW: Phone: +61 (52) 277-3116, email: tiffany.walsh@deakin.edu.au

AuBP1	Au	Ag	**AuBP2**	Au	Ag	**AgBP1**	Au	Ag†	**AgBP2**	Au	Ag
W	84	39	**W**	77	7	**T**	7	4	**E**	14	4
A	48	26	**A**	8	7	**G**	7	4	**Q**	23	20
G	66	48	**L**	9	44	**I**	26	10	**L**	41	8
A	58	22	**R**	61	54	**F**	33	7	**G**	68	41
K	22	22	**R**	46	4	**K**	27	8	**V**	39	3
R	92	59	**S**	16	15	**S**	31	33	**R**	74	32
L	46	19	**I**	45	10	**A**	55	34	**K**	22	8
V	39	47	**R**	32	40	**R**	75	51	**E**	37	7
L	49	36	**R**	11	30	**A**	41	35	**L**	37	1
R	77	46	**Q**	11	58	**M**	84	39	**R**	68	9
R	85	63	**S**	32	33	**R**	63	26	**G**	47	27
E	50	6	**Y**	64	16	**A**	45	38	**V**	15	1

Table S1: Summary of contact residue data for each of the four sequences, AuBP1, AuBP2, AgBP1, AgBP2, adsorbed at either the Au or Ag aqueous interfaces. For each residue, we give the percentage of the entire REST MD reference trajectory (%) that each residue is determined to be in contact with the surface. All trajectories were of 15 x 10^6 MD steps, except for †, which was 20 x 10^6 MD steps.

Cluster Rank	AuBP1 : 53 (104)	AuBP2 : 98 (121)	AgBP1 :118 (198†)	AgBP2 : 112 (144)
1	21.2 (15.9)	30.2 (40.9)	21.6 (12.3)	23.8 (23.3)
2	15.7 (12.0)	17.3 (4.5)	11.9 (6.7)	20.1 (10.0)
3	13.8 (11.1)	7.5 (4.2)	11.3 (5.5)	11.9 (9.9)
4	12.8 (8.8)	7.4 (4.2)	6.6 (4.8)	6.9 (4.4)
5	6.0 (7.5)	3.9 (3.8)	5.6 (3.6)	4.6 (3.7)
6	5.7 (5.1)	3.4 (3.6)	4.3 (3.5)	4.0 (3.5)
7	3.3 (4.9)	3.4 (3.1)	3.3 (3.4)	3.9 (3.4)
8	2.8 (3.2)	3.3 (2.9)	3.0 (2.9)	2.5 (2.3)
9	2.3 (2.6)	2.2 (2.8)	2.6 (2.7)	1.7 (2.3)
10	2.1 (2.4)	2.0 (2.8)	2.3 (2.6)	1.5 (2.2)

Table S2: Clustering data for each of the four peptide sequences AuBP1, AuBP2, AgBP1, AgBP2, adsorbed on Au and Ag. Ag-adsorbed data are given in parentheses. The table header gives the total number of clusters, table entries give the percentage population of each cluster for the Top 10 most populated clusters. † indicates analysis was carried out over the entire extended 20 ns trajectory.

(a)

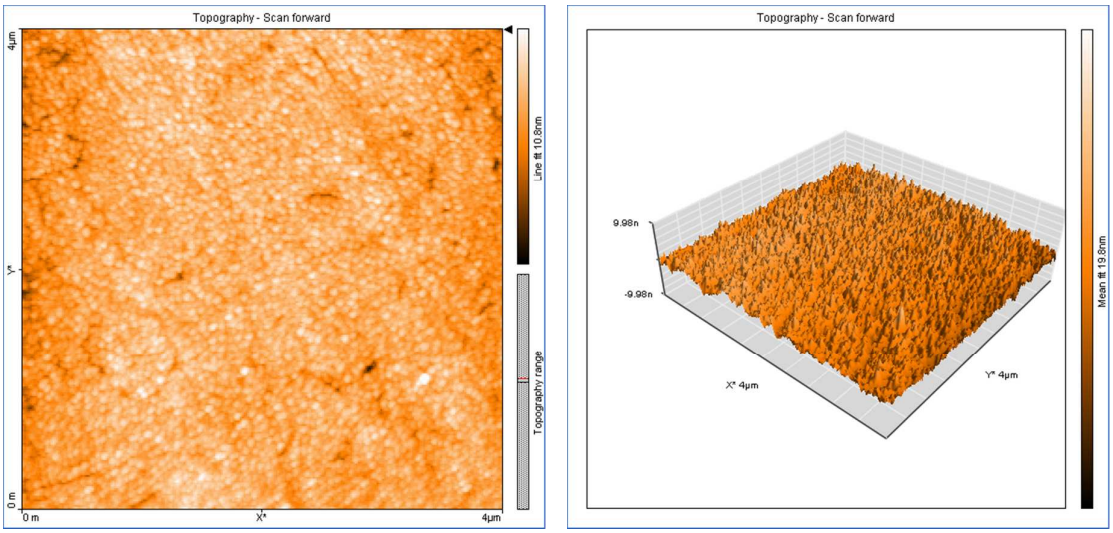

(b)

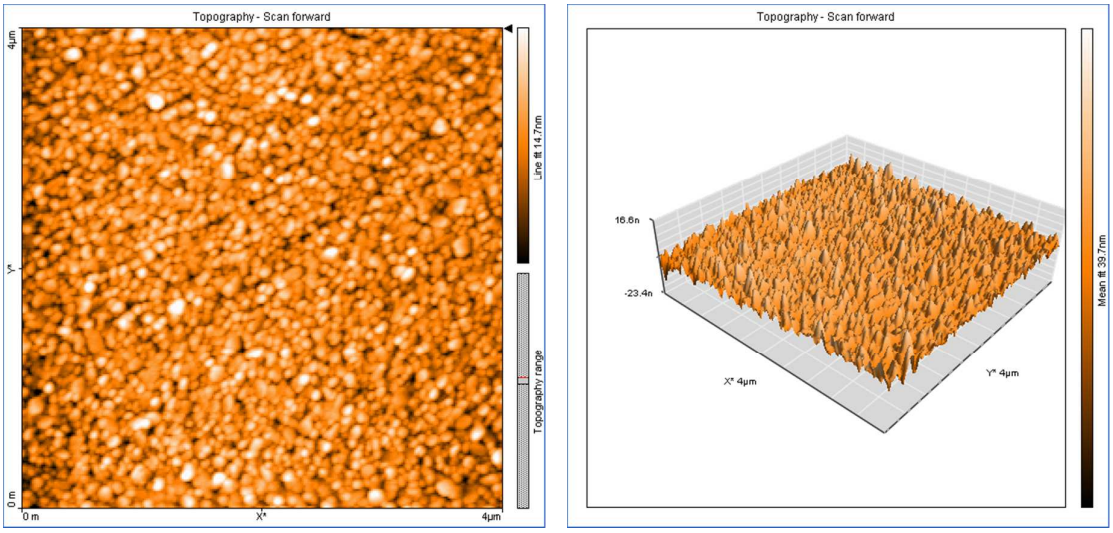

Figure S1. Tapping-mode AFM images of representative (a) Au and (b) Ag sensors to characterize the local surface roughness of the surface prior to peptide adsorption. The RMS roughness was 1.1 nm for the Au sensor and 2.4 nm for the Ag sensor over the areas shown in images (a) and (b), respectively.

(a)

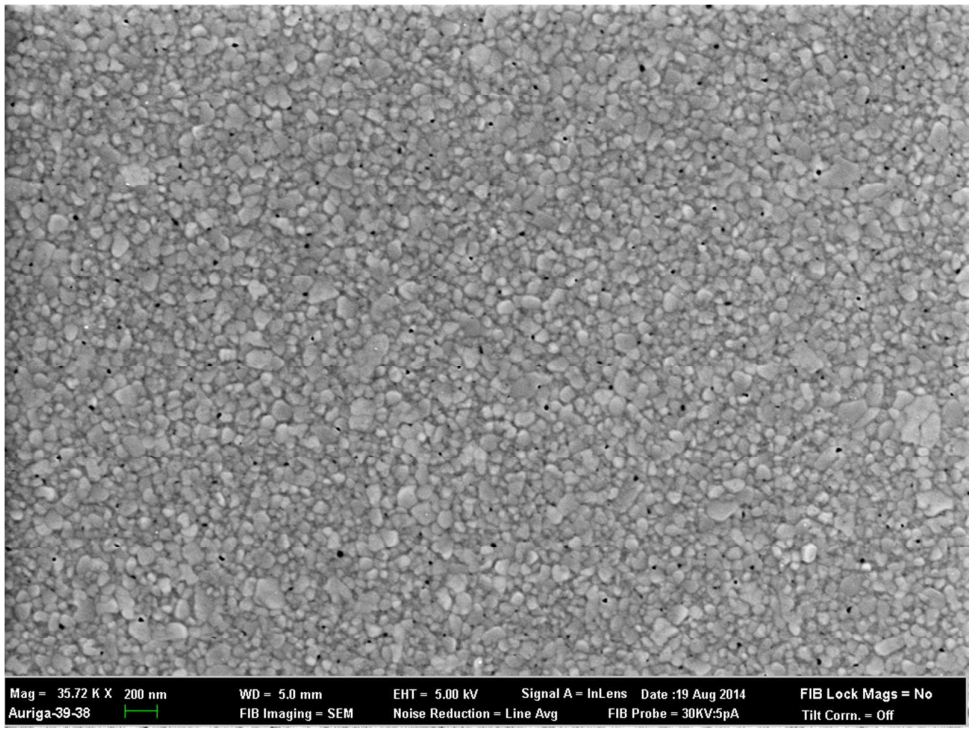

(b)

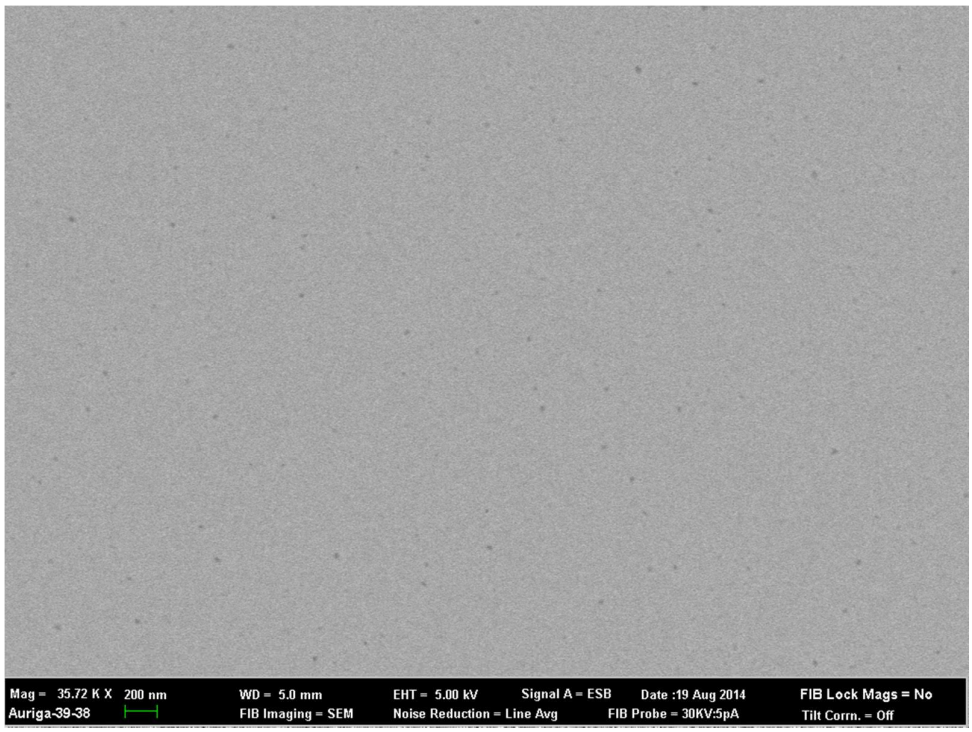

Figure S2. SEM images of a QCM sensor after Ag-coating with (a) secondary electron detection, providing topographical contrast and showing granular roughness consistent with the AFM imaging in Figure S1, and (b) backscattered electron imaging which provides elemental contrast, showing that the Ag film uniformly covers the underlying Au surface.

(a)

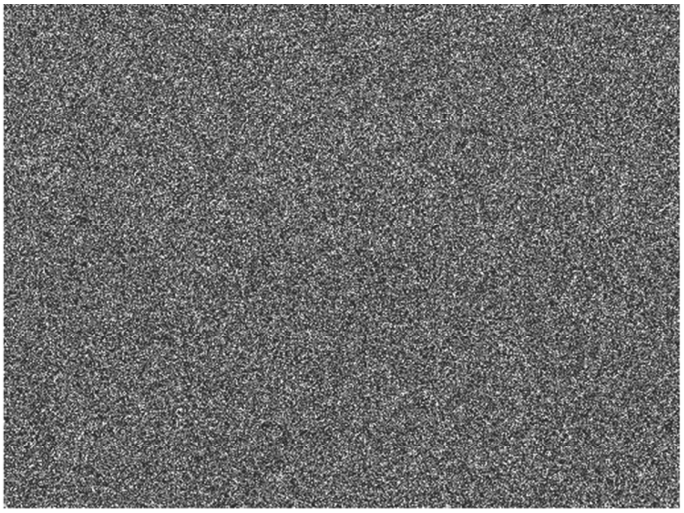

Ag La1

(b)

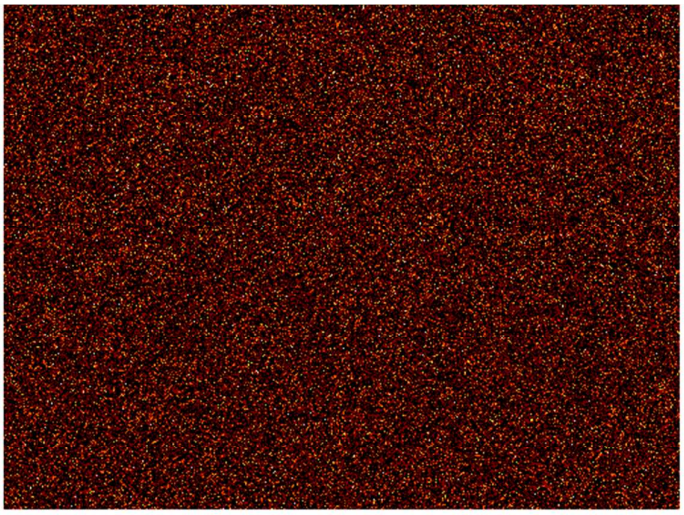

Au Ma1

Figure S3. EDS elemental maps of (a) Ag and (b) Au for the Ag-coated QCM sensor for which SEM images were shown on Figure S2. The imaged area is approximately 4 μm by 3 μm. The overall composition of the imaged area from EDS analysis was approximately 94% Ag, 6% Au. The visibility of Au in EDS simply reflects the fact that the sampling depth at the lowest possible electron energy (5 keV) is greater than the Ag film thickness. However the imaging above shows that the composition is uniform over the imaged region.

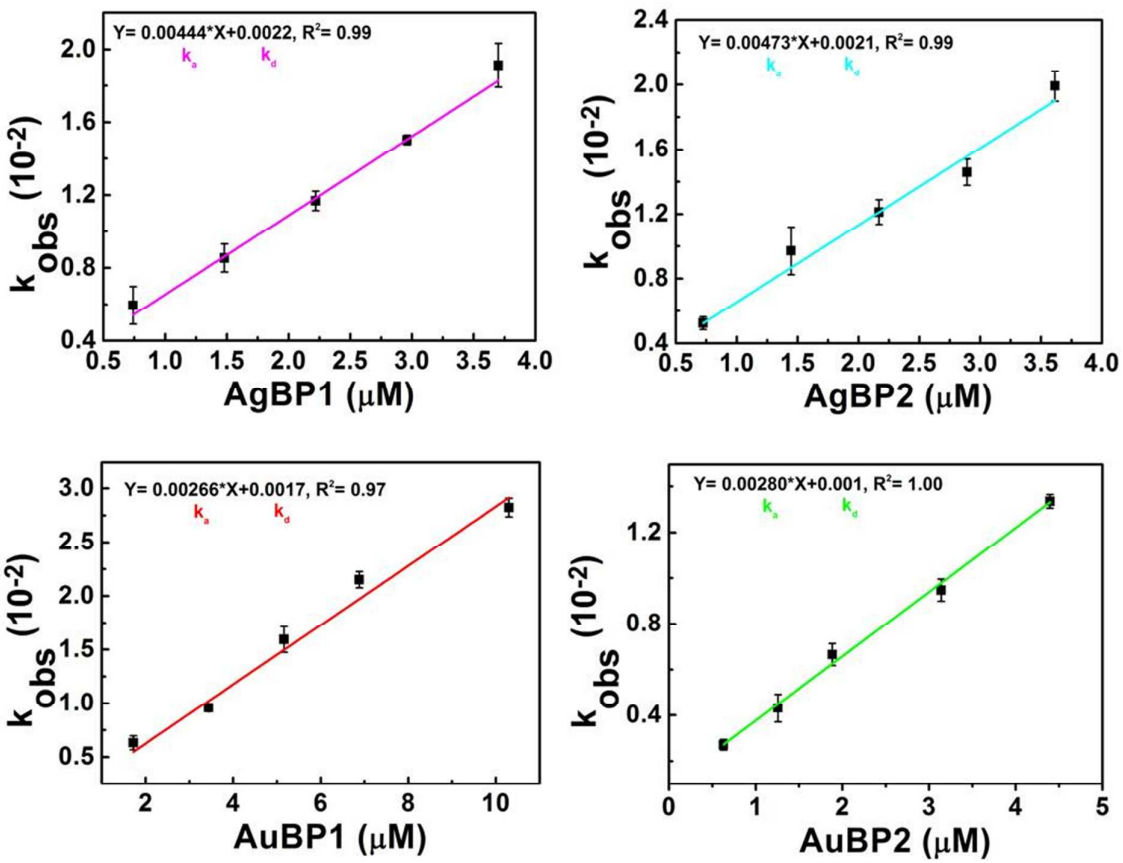

Figure S4. Plot of k_{obs} values *vs*. peptide concentration of AgBP1, AgBP2, AuBP1 and AuBP2 respectively. The k_{obs} values were obtained through Langmuir fitting from data shown in Figure 1 of the main text.

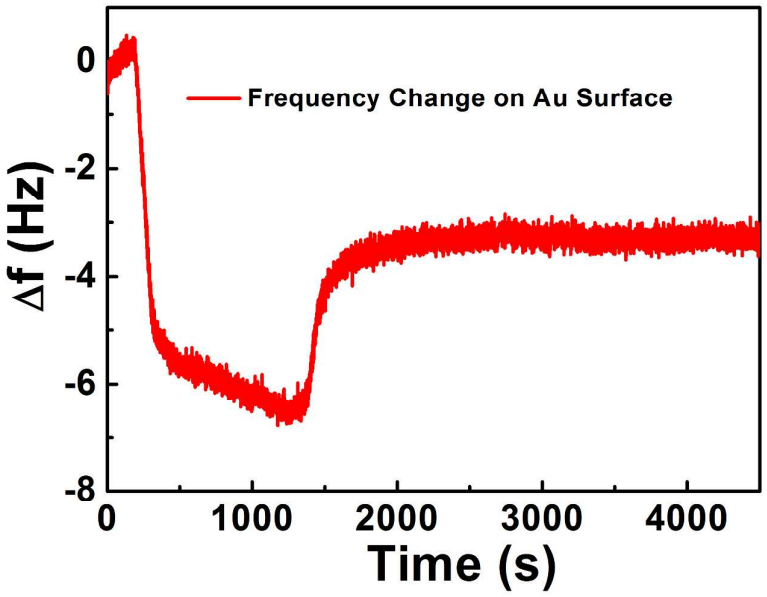

Figure S5. Peptide desorption from the Au sensor surface. For this analysis, monitoring of peptide binding (AuBP1) to the Au sensor was studied at a concentration of 5.0 μg/mL. Upon binding saturation, water was flowed over the interface leading to desorption. Complete desorption was not observed; ~50% of the initially bound AuBP1 remained adsorbed.

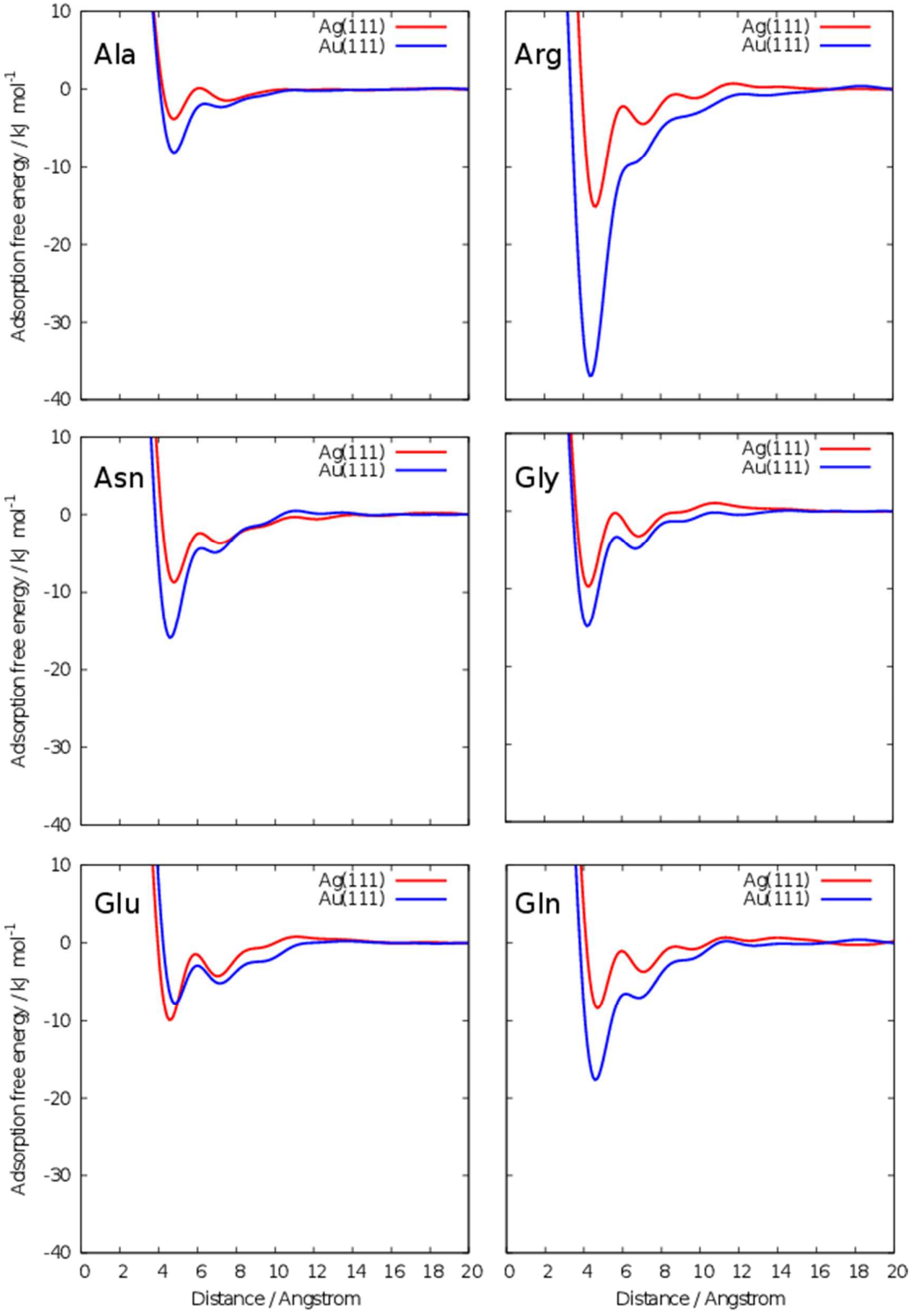

Figure S6: Calculated adsorption free energies for the amino acids Ala, Arg, Asn, Gly, Glu and Gln, at the aqueous metal interface, as a function of separation between the amino acid center-of-mass and the surface.

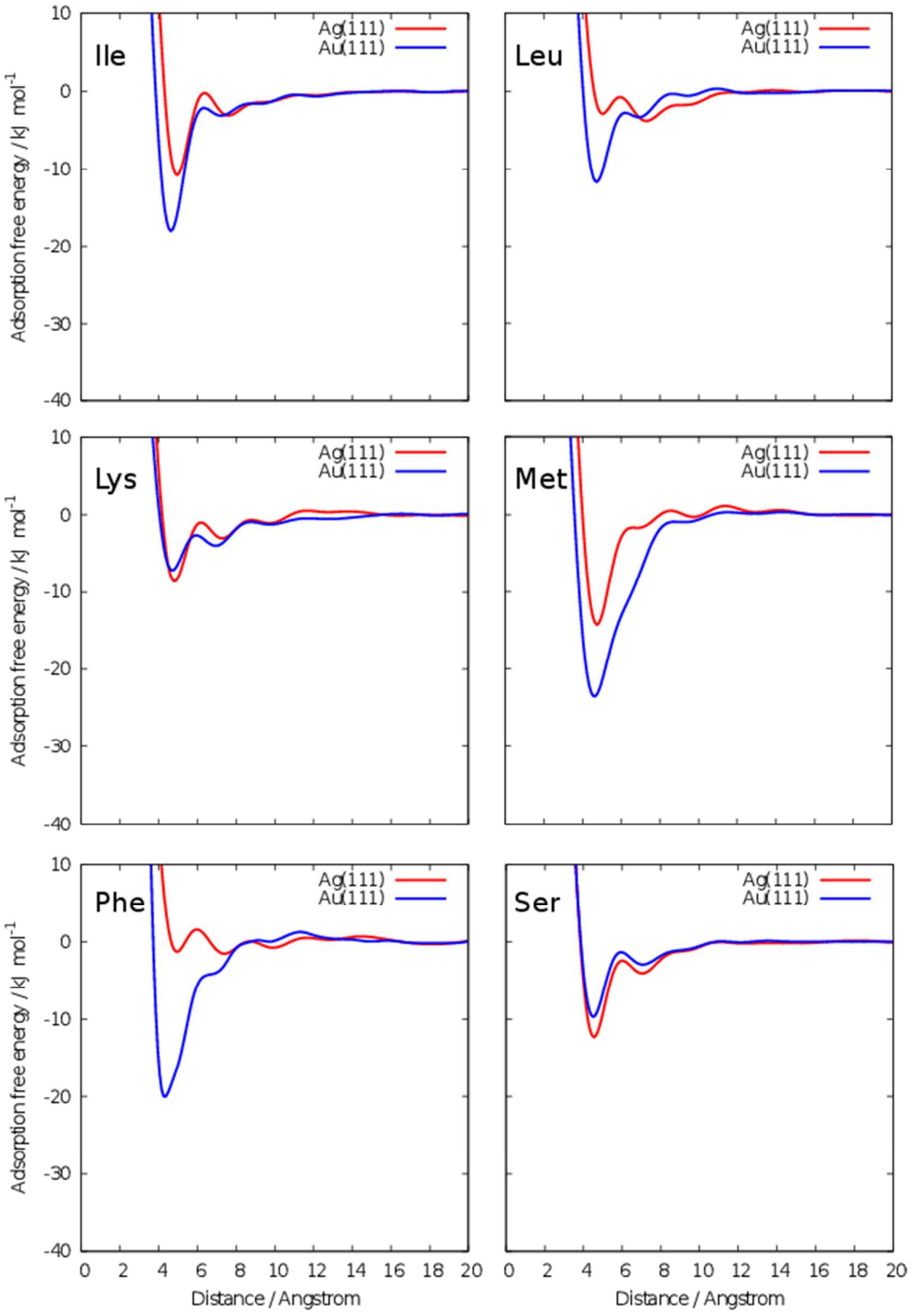

Figure S7: Calculated adsorption free energies for the amino acids Ile, Leu, Lys, Met, Phe and Ser, at the aqueous metal interface, as a function of separation between the amino acid center-of-mass and the surface.

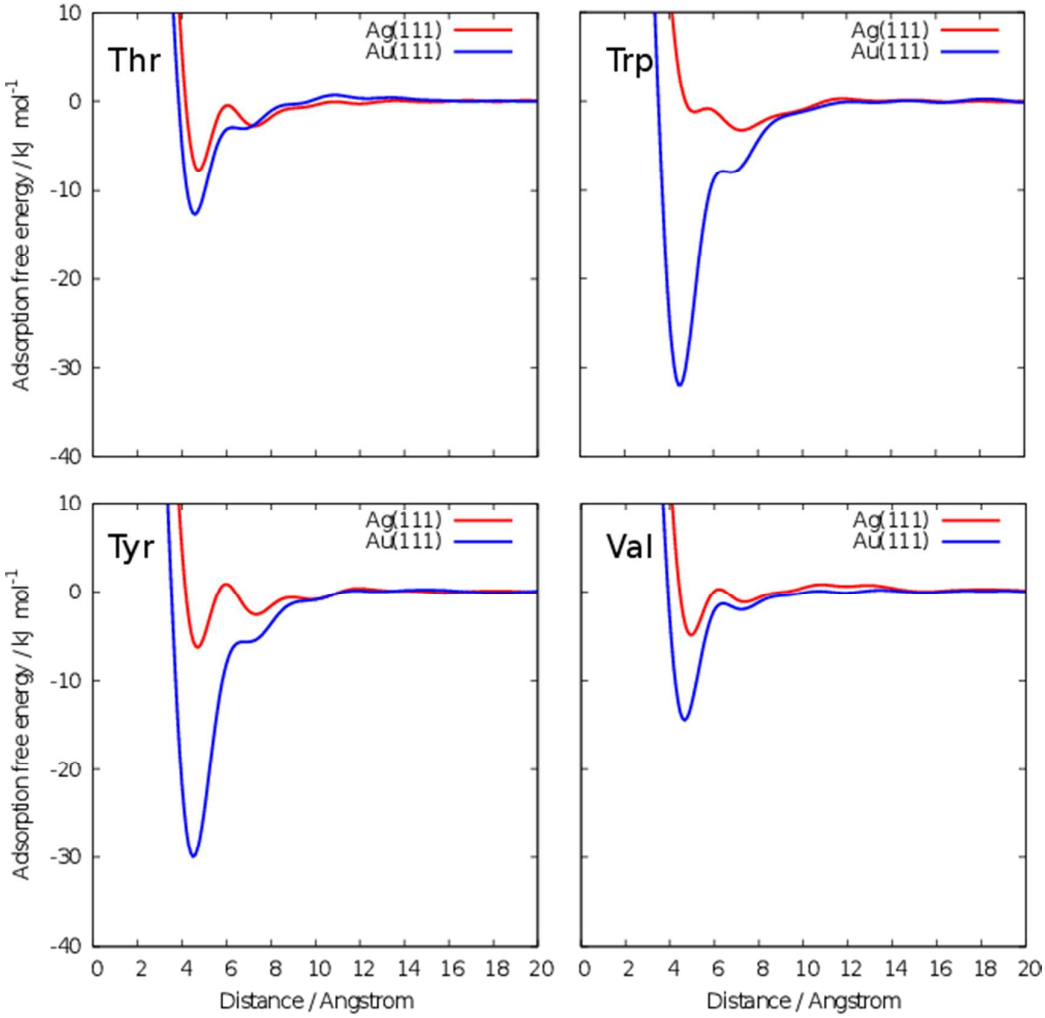

Figure S8: Calculated adsorption free energies for the amino acids Thr, Trp, Tyr and Val, at the aqueous metal interface, as a function of separation between the amino acid center-of-mass and the surface.

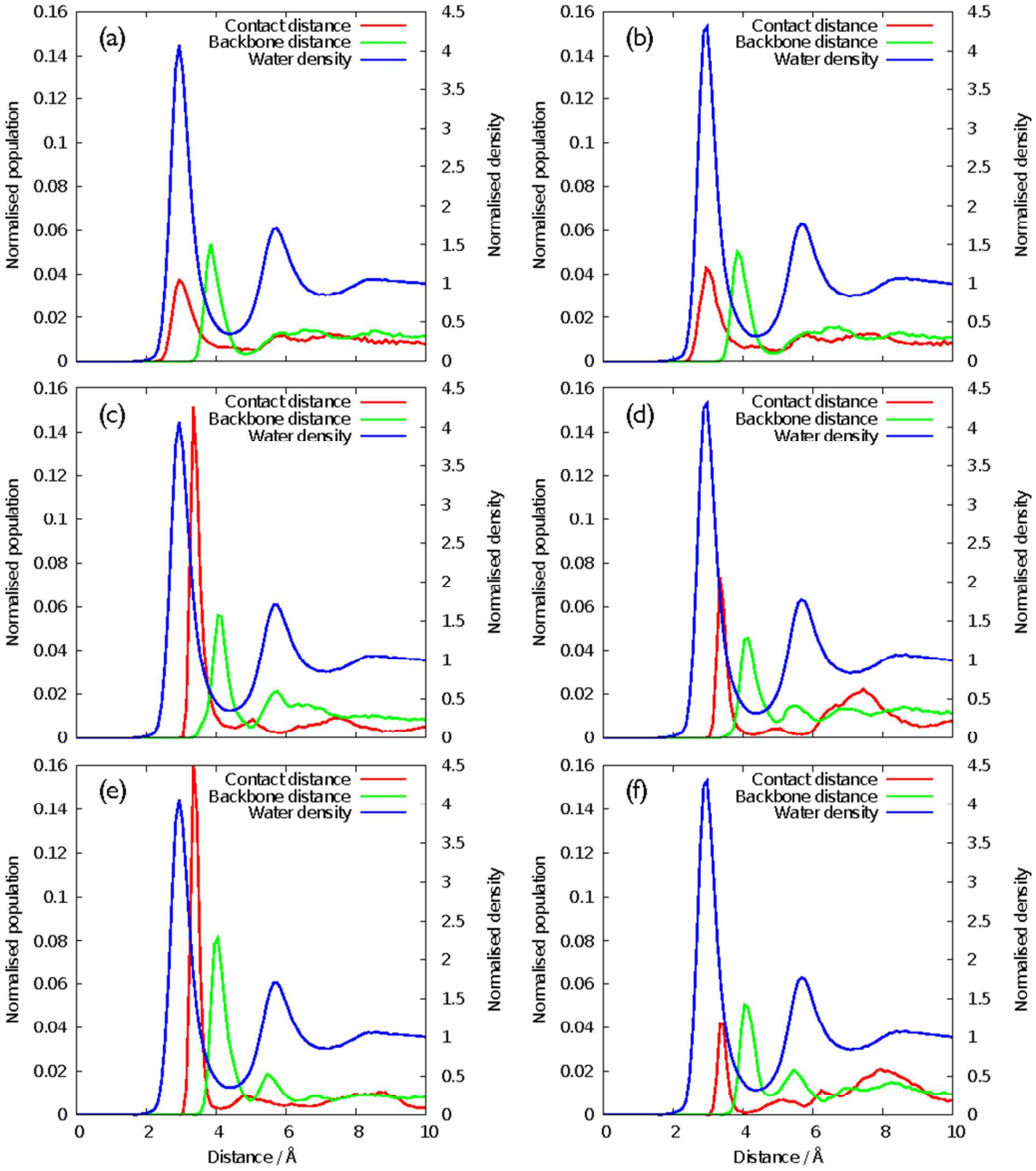

Figure S9: Calculated relative proportion of contact mode in the adsorbed state, where "Contact Distance" refers to the side chain-surface distance, and "Backbone distance" refers to the backbone-surface distance. (a) Ser on Au(111), (b) Ser on Ag(111), (c) Tyr on Au(111), (d) Tyr on Ag(111), (e) Trp on Au(111), (f) Trp on Ag(111). In each case, the water density profile perpendicular to the metal surface is also shown for reference.

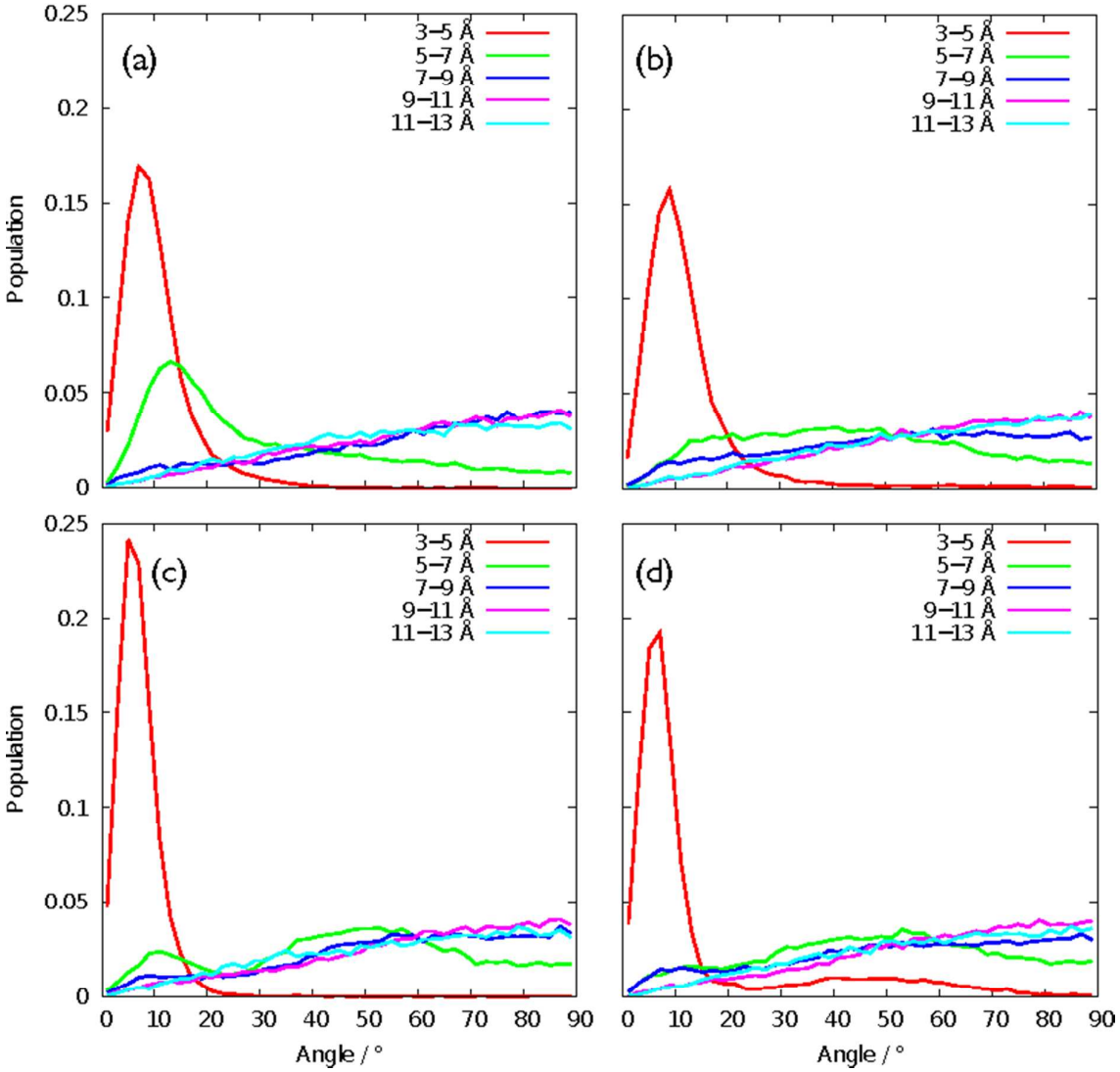

Figure S10: Calculated population of the side-chain ring orientation relative to the surface when in the adsorbed state, as a function of amino acid – surface distance. (a) Tyr on Au(111), (b) Tyr on Ag(111), (c) Trp on Au(111), (d) Trp on Ag(111).

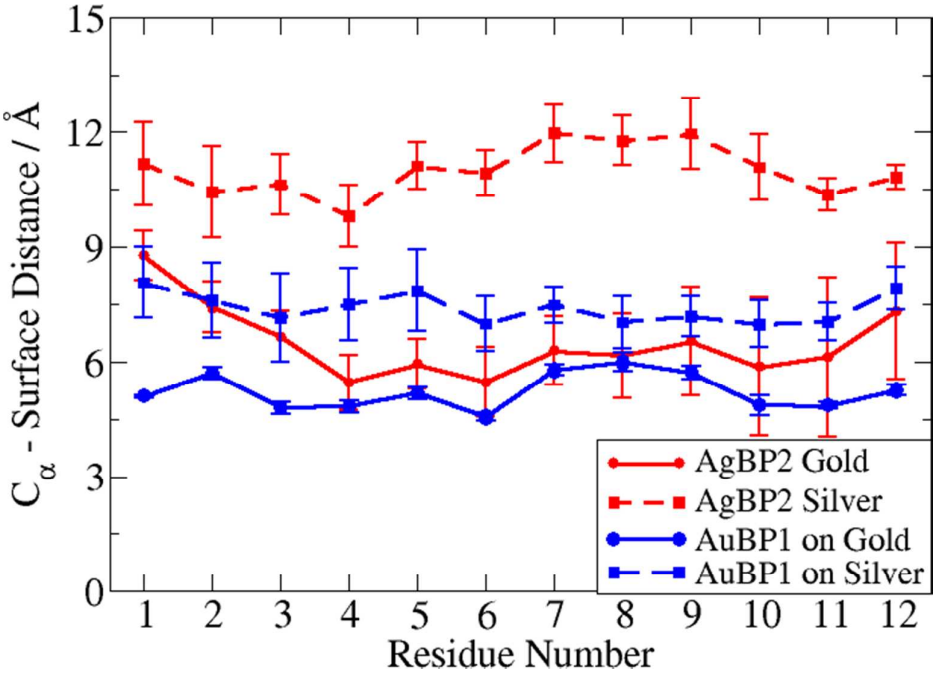

Figure S11: Average distance between each C(α) atom in a given peptide sequence and the metal surface, taken from the reference replica REST MD simulation trajectories. AuBP1 is shown for contrast; plots for AuBP2 and AgBP1 are similar to AuBP1.

Additional Computational Details:

REST Simulations: System setup: Each system (8 systems in total) comprised one 5-layer Ag or Au slab presenting the (111) surface on both sides of the slab, one peptide chain, ~6600 water molecules, and, as required, counter-ions (in the form of Na^+ and Cl^- ions) to ensure overall charge neutrality of the simulation cell. Each peptide was modelled with the zwitterionic form of the N- and C-termini (*i.e.* no capping groups), consistent with the experimentally synthesized peptides. Each residue in each peptide was assigned a protonation state consistent with a solution pH of ~7. We used an orthorhombic periodic cell; the gold slab had lateral dimensions 58.6 Å x 60.9 Å, with an inter-slab spacing perpendicular to the slab surface in excess of 55 Å (such that the perpendicular dimension of the cell was 67.6 Å). The height of the cell was adjusted such that the density of liquid water in the central region between the slabs was consistent with the liquid water density at room temperature and ambient pressure. Periodic boundary conditions were applied in all three dimensions. All simulations were performed in the Canonical (*NVT*) ensemble, at a temperature of 300K, maintained using the Nosé-Hoover thermostat[1-3], with a coupling constant of τ = 0.4 ps. Newton's equations of motion were solved using the leapfrog algorithm[4] with an integration time-step of 1fs. Coordinates and velocities were saved every 1000 steps (1ps). Long-ranged electrostatic interactions were treated using Particle-mesh Ewald (PME), with a cut-off at 11 Å, whereas a force-switched cut-off, starting at 9 Å and ending at 10 Å was used for Lennard-Jones non-bonded interactions.

The recently-derived polarizable GolP-CHARMM force-field[5] was used to model the interactions between the water (described with the modified TIP3P force-field[6,7]) and the Au slab. The AgP-CHARMM force-field[8] was used for the Ag slab. The peptide was described using the CHARMM22* force-field[9, 10]. The rigid-rod-dipole method for gold atom polarization was implemented, as per previous versions of the GolP force-field[11]. All metal atoms in the slab were held fixed in space during these simulations, with only the metal atom dipoles able to freely rotate. Random initial dipole positions were used throughout. Our recent tests indicate that there is very little difference between binding free energies obtained using a rigid substrate, vs. using a slab where all atoms can move.[12]

REST Details: Our implementation of REST uses the replica exchange and free energy perturbation theory codes within Gromacs 4.5.5[13]. Briefly, for the systems studied in this work, the potential energy of each replica, *j*, was scaled according to:

$$V_j(X) = \frac{\beta_j}{\beta} V_{pp}(X) + \sqrt{\frac{\beta_j}{\beta}} V_{ps}(X) + V_{ss}(X)$$

where V_{pp} is the intra-peptide, V_{ps} is the peptide-water and peptide-surface, and, V_{ss} is the surface-surface, surface-water and water-water potential energies of the system, X. β and β_j are the inverse of the system and "effective" temperatures of replica *j*, and are related via the parameter λ_j:

$$\beta_j = \beta(1 - \lambda_j) + \beta_H \lambda_j$$

where $0 \leqslant \lambda_j \leqslant 1$, and β_H corresponds to the highest "effective" temperature. We refer readers to the work of Terakawa *et al.*[14] and Wright *et al.*[15] for further basic details of REST simulations in general.

In our REST simulations, we spanned an effective temperature window of 300-430K with 16 replicas. The initial configurations for each replica cover a range of secondary structures, including α-helix, β-turn, polyproline II and random coil conformations. The peptide structures were initially placed so that at least one peptide atom was within ~7Å distance from the top surface of the metal slab. The 16 values of lambda used to scale our force-field were:

λ_j = 0.0000, 0.057, 0.114, 0.177, 0.240, 0.310, 0.382, 0.458, 0.528, 0.597, 0.692, 0.750, 0.803, 0.855, 0.930, 1.0000.

Following Wright *et al.*[15], only the bond-stretching, dihedral, and non-bonded terms of the intra-peptide potential were scaled for each replica. Before initiating the REST run, initial configurations were equilibrated at their target potential for 0.5 ns, with no exchange moves attempted in this period. The average probability of an exchange attempt being accepted was approximately 0.7, with the interval between exchange attempts set to 1000 MD steps (every 1 ps). All production REST simulations were run for a total of 15×10^6 MD steps (15 ns), except for the AgBP1/Ag(111) system, which required 20×10^6 MD steps to reach satisfactory equilibration. In Figure S10, we show an example of evidence used to determine sample equilibration, namely the number of clusters vs. MD steps for the unscaled, reference replica (λ = 0.000). These data show in this particular case that the number of new, different structures (consistent with our clustering RMSD cut-off in backbone positions) has plateaued at around 10ns.

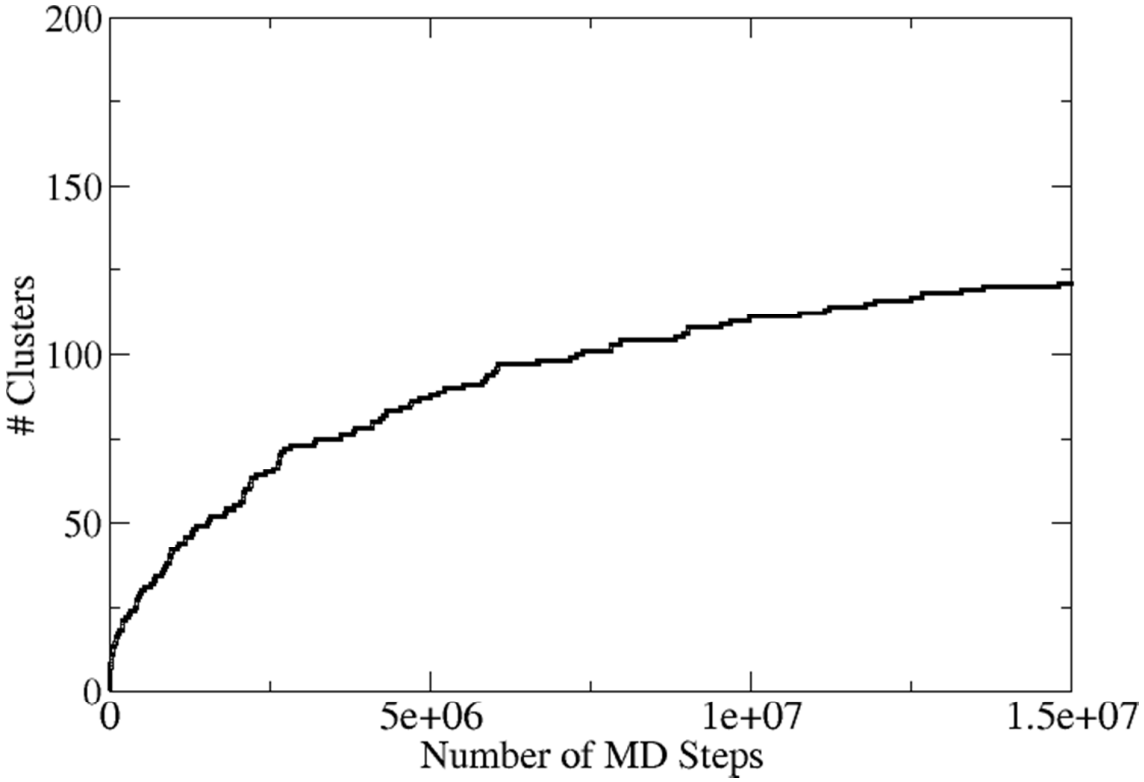

Figure S12: Number of clusters as a function of MD steps, shown for the AuBP2 sequence reference REST trajectory, adsorbed at the aqueous Ag(111) interface.

Contact Residue Scoring:

We used the free energies of binding for all 20 naturally-occurring amino-acids, as reported in Figure 3 (main text), as a basis for assigning a score to each assigned contact residue, for each peptide sequence (see Table 1, main text). We drew the boundaries between strong-, medium- and weak-binding amino-acids, such that weak had $\Delta A_{amino} > -15$ kJ mol-1, medium had -15 kJ mol-1 $> \Delta A_{amino} > -25$ kJ mol-1 and strong had $\Delta A_{amino} < -25$ kJ mol-1. The set of strong-binding ("high") amino-acids was [Tyr, Trp, Phe, Met, Arg, His], the set of medium-binding ("middle") amino-acids was [His, Lys, Thr, Gln, Asn, Pro] and the set of weak-binding ("low") amino-acids was [Asp, Leu, Ile, Val, Gly, Ser, Ala, Glu]. "High" contact residues were assigned a score of 4, "Middle" contact residues were assigned a score of 3, and "Low" residues were assigned a score of 2.

The total score for each sequence was determined from the sum of the contact residue scores. For example, AuBP1 adsorbed on Au(111) has 5 contact residues (where "contact residue" is defined as having 60% surface contact or greater – see Table S1): Trp, Gly, Arg, Arg, Arg – giving a total score of 4+2+4+4+4=18.

We assign peptides with total scores < 10 the designation "Weak", with "Medium" having $10 <$ score < 15, and with "Strong" having a score of > 15.

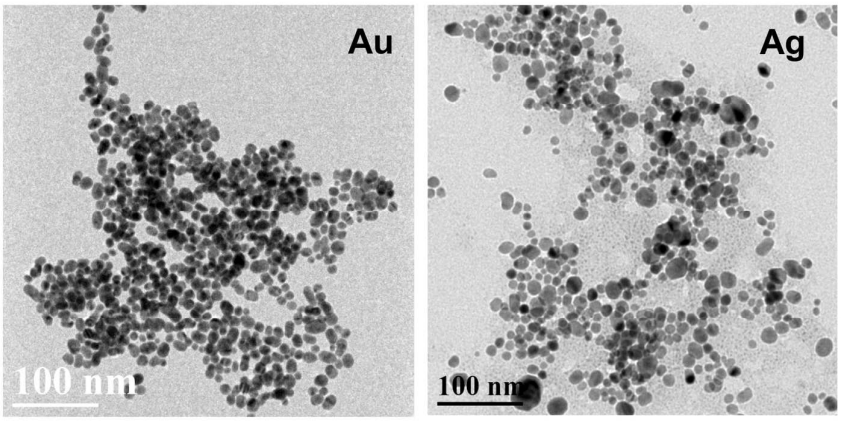

Figure S13. Control synthesis of Au (left) and Ag (right) nanoparticles in the absence of peptide. Nanostructures were observed with sizes of 11.5 ± 1.7 nm for Au and 12.7 ± 4.2 nm for Ag. These nanoparticles are significantly more polydisperse in size and morphology than materials fabricated using the materials-binding peptides.

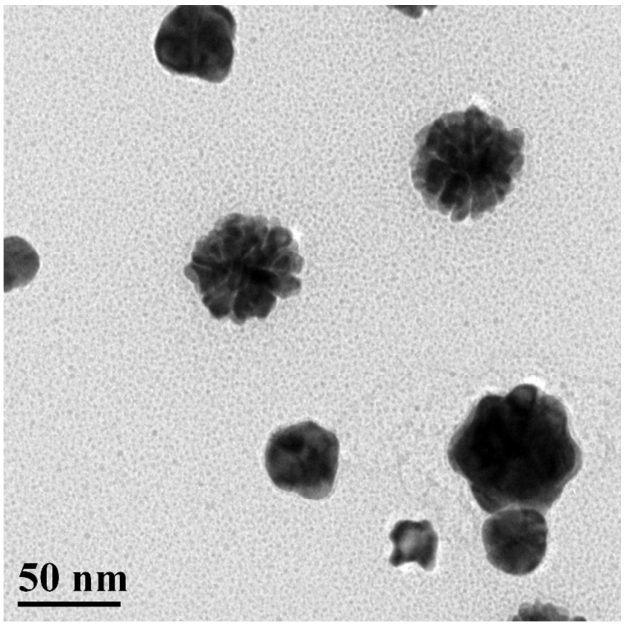

Figure S14. TEM image of the Au nanoparticles prepared using the AuBP2 peptide employing ascorbic acid as the reductant. Under these conditions, large, polycrystalline, porous materials were observed.

References:

1. Nose, S., A Molecular-Dynamics Method for Simulations in the Canonical Ensemble. *Mol. Phys.* 1984, 52, 255-268.
2. Nose, S., A Unified Formulation of the Constant Temperature Molecular-Dynamics Methods. *J. Chem. Phys.* 1984, 81, 511-519.
3. Hoover, W. G., Canonical Dynamics - Equilibrium Phase-Space Distributions. *Phys. Rev. A* 1985, 31, 1695-1697.
4. Hockney, R. W.; Goel, S. P.; Eastwood, J. W., Quiet High-Resolution Computer Models of a Plasma. *J. Comput. Phys.* 1974, 14, 148-158.
5. Wright, L. B.; Rodger, P. M.; Corni, S.; Walsh, T. R., GolP-CHARMM: First-Principles Based Force Fields for the Interaction of Proteins with Au(111) and Au(100). *J. Chem. Theory Comput.* 2013, 9, 1616-1630.
6. Jorgensen, W. L.; Chandrasekhar, J.; Madura, J. D.; Impey, R. W.; Klein, M. L., Comparison of Simple Potential Functions for Simulating Liquid Water. *J. Chem. Phys.* 1983, 79, 926-935.
7. Neria, E.; Fischer, S.; Karplus, M., Simulation of Activation Free Energies in Molecular Systems. *J. Chem. Phys.* 1996, 105, 1902-1921.
8. Z. E. Hughes, L. B. Wright and T. R. Walsh, Biomolecular Adsorption at Aqueous Silver Interfaces: First-Principles Calculations, Polarizable Force-Field Simulations, and Comparisons with Gold. *Langmuir* 2013, 29, 13217-13229.
9. MacKerell, A. D.; Bashford, D.; Bellott, M.; Dunbrack, R. L.; Evanseck, J. D.; Field, M. J.; Fischer, S.; Gao, J.; Guo, H.; Ha, S.; Joseph-McCarthy, D.; Kuchnir, L.; Kuczera, K.; Lau, F. T. K.; Mattos, C.; Michnick, S.; Ngo, T.; Nguyen, D. T.; Prodhom, B.; Reiher, W. E.; Roux, B.; Schlenkrich, M.; Smith, J. C.; Stote, R.; Straub, J.; Watanabe, M.; Wiorkiewicz-Kuczera, J.; Yin, D.; Karplus, M., All-atom empirical potential for molecular modeling and dynamics studies of proteins. *J. Phys. Chem. B* 1998, 102, 3586-3616.
10. Piana, S.; Lindorff-Larsen, K.; Shaw, D. E., How Robust Are Protein Folding Simulations with Respect to Force Field Parameterization? *Biophys. J.* 2011, 100, L47-L49.
11. Iori, F.; Di Felice, R.; Molinari, E.; Corni, S., GoIP: An Atomistic Force-Field to Describe the Interaction of Proteins With Au(111) Surfaces in Water. *J. Comput. Chem.* 2009, 30, 1465-1476.
12. Wright, L. B.; Freeman, C. L.; Walsh, T. R., Adsorption at the Aqueous (011) alpha-quartz Interface: Is Surface Flexibility Important? *Mol. Simulat.* 2013, 39, 1093-1102.
13. Hess, B.; Kutzner, C.; van der Spoel, D.; Lindahl, E., GROMACS 4: Algorithms for highly efficient, load-balanced, and scalable molecular simulation. *J. Chem. Theory Comput.* 2008, 4, 435-447.
14. Terakawa, T.; Kameda, T.; Takada, S., On Easy Implementation of a Variant of the Replica Exchange with Solute Tempering in GROMACS. *J. Comput. Chem.* 2011, 32, 1228-1234.
15. Wright, L. B.; Walsh, T. R., Efficient conformational sampling of peptides adsorbed onto inorganic surfaces: insights from a quartz binding peptide. *Phys. Chem. Chem. Phys.* 2013, 15, 4715-4726.